3D modeling and RNA-based therapeutics for Dutch-type cerebral amyloid angiopathy

Daoutsali, E.

CHAPTER 5

ABNORMAL CELLULAR LOCALIZATION OF D-CAA APP CAN BE PARTIALLY NORMALIZED BY GENERATION OF A SHORTER APP ISOFORM (APPΔ17)

Elena Daoutsali[1], Barry A. Pepers[1], Linda M. van der Graaf[1] and Willeke M.C. van Roon-Mom[1]

[1] Department of Human Genetics, Leiden university Medical Center, Leiden, the Netherlands

submitted to Cellular and Molecular Neurobiology

ABSTRACT

Dutch-type cerebral amyloid angiopathy (D-CAA) is a rare autosomal dominant brain disease that is characterized by intracerebral hemorrhagic strokes and vascular dementia. The disease is caused by a point mutation in exon 17 of the amyloid precursor protein (APP) gene that leads to an amino acid substitution within the Aβ domain of APP, resulting in an Aβ peptide that is more prone to aggregation. Recently, we showed that an antisense oligonucleotide (AON) approach targeting exon 17, results in a shorter APP isoform (APPΔ17) and a reduction of Aβ40 levels. This RNA-modifying therapy removes both the D-CAA mutation and part of the APP transmembrane domain. The transmembrane domain is important for APP localization, which in turn is important for APP cleavage. The aim of this study was to determine differences in APP localization between wild type, D-CAA APP and the APPΔ17 isoform that is formed with our APP targeting AON, looking at endogenously expressed APP in neuronally differentiated patient-derived induced pluripotent stem cells (iPSCs). The D-CAA mutation caused aberrant colocalization of the APP C-terminal fragment (CTF) with Golgi and early endosomes in neuronally differentiated D-CAA iPSCs compared to control iPSCs. To validate these findings and examine localization of the shorter APPΔ17 isoform, we transiently transfected neuroblastoma cells with plasmids containing moxGFP/mScarlet dual tagged wild-type APP, D-CAA APP or APPΔ17. D-CAA APP CTFs exhibited increased localization with early endosomes and lysosomes that was restored in APPΔ17. These results suggest that aberrant cellular APP localization in D-CAA could play a role in APP cleavage potentially altering downstream biological processes and contributing to D-CAA neuropathology. This aberrant localization is normalized when the shorter APPΔ17 isoform is expressed indicating that the antisense oligonucleotide approach targeting exon 17 of APP could improve disease signatures.

INTRODUCTION

Dutch-type cerebral amyloid angiopathy (D-CAA) is a monogenic form of cerebral amyloid angiopathy (CAA). This hereditary neurodegenerative disease is caused by a point mutation at codon 693 of the amyloid precursor protein (APP) gene (1-3). The G to C change (NM_000484.3(APP):c.2077G>C) leads to substitution of glutamic acid by glutamine (NP_000475.1:p.Glu693Gln) within the amyloid beta (Aβ) domain of APP (E22Q). In D-CAA, Aβ accumulates in the cerebral leptomeningeal arteries and cortical arterioles causing degeneration of vascular smooth muscle cells and intracerebral hemorrhage (ICH) (4).

APP is a type I transmembrane glycoprotein and is widely studied due to its involvement in the generation of the toxic Aβ peptides in Alzheimer's disease (AD) and CAA (5, 6). It is cleaved via two pathways that were named based on the absence or presence of the Aβ peptide, the non-amyloidogenic and the amyloidogenic pathway respectively. Cleavage of APP first by α-secretase leads to the production of a large soluble APP derivative termed sAPPα and a C-terminal fragment (CTF) named CTFα or C83 that is sequentially cleaved by γ-secretase to generate a small 3kDa fragment (P3) and the APP-intracellular domain (AICD). The sAPPα fragment has been shown to have neurotrophic and neuroprotective properties (7-10). In the amyloidogenic pathway, initial cleavage with β-secretase generates the soluble APPβ (sAPPβ) fragment and CTFβ or C99 that is cleaved by γ-secretase and produces the Aβ peptide and AICD (11). sAPPβ does not share the neuroprotective properties of sAPPα, however it was found to be important in synapse pruning (12). γ-Secretase can cleave APP in multiple sites thus generating Aβ fragments of various lengths. In D-CAA the predominant Aβ peptide is 40aa long (13). The AICD fragment that is produced both from the amyloidogenic and non-amyloidogenic pathways, contains several motifs that are crucial for interactions with other proteins (e.g Fe65) that translocate AICD to the nucleus and activate transcription of target genes (14, 15).

For proper APP cleavage, trafficking through and localization within the cell is important (16-18). APP traffics along the secretory, endocytic and recycling pathways. It is synthesized in the membrane-bound polysomes and translocates to the endoplasmic reticulum (ER). The majority of APP is then transported to the Golgi apparatus where it is glycosylated and exits the Golgi apparatus at the trans-Golgi network (TGN). Around 10% of APP reaches the plasma membrane where the high abundance of α-secretase makes it the predominant site for non-amyloidogenic processing of APP. The amyloidogenic pathway is widely considered to occur in late Golgi compartments and the endolysosomal system. More specific, β-secretase cleavage occurs in the TGN and endosomes, while γ-secretase cleavage has been reported to occur in the TGN, endosomes and lysosomes (19, 20). Alternatively, APP can rapidly traffic from the cell surface to lysosomes, bypassing endosomes, where it is processed by γ-secretase to produce Aβ and AICD (21). Since the different APP cleavage fragments have different functions, a change in cellular localization could have consequences in APP cleavage and influence downstream cellular processes (22, 23).

More than 50% of APP disease-causing mutations are found in the transmembrane (TMD) and juxtamembrane domains (JMD), close or distant from the secretase cleavage sites (24-28). The area of the JMD immediately following the α-secretase cleavage site location (K687) contains a large

number of APP mutations that seem to play important roles in determining the ratio of short versus long Aβ peptides (29). The D-CAA mutation is located in this domain and it was recently shown that mutations in the JMD of APP differentially influence APP processing and lead to reduction of the secretion of Aβ40 and Aβ42 peptides and generation of shorter Aβ peptides (30). Furthermore, mutations in residues K28 and S26 that are also part of the JMD, have been shown to reduce Aβ secretion without affecting AICD production (25, 31).

In a previous study by our group we confirmed equal levels of Aβ40 in control and D-CAA induced pluripotent stem cell (iPSC)-derived neuronal cells and that these Aβ40 levels could be reduced by modulating splicing of APP pre-mRNA with antisense oligonucleotides (AON). The AON excluded exon 17 from the APP pre-mRNA resulting in the removal of the Dutch mutation and the γ-secretase cleavage site from the modified APP protein. This leads to the generation of a new protein isoform, named APPΔ17 (32). Since exon 17 encodes for part of the JMD and TMD of APP, APP localization and trafficking could be affected by the D-CAA mutation and normalized by removing the D-CAA mutation containing exon.

In the present study, we first investigated the endogenous cellular localization of wild-type (wt) and D-CAA APP in control and D-CAA iPSC-derived neuronal cells, using N- and C-terminal specific APP antibodies, in combination with antibodies against ER, Golgi and endosomes, where we showed higher co-localization of D-CAA CTF APP within Golgi and endosomes. Next, we investigated the co-localization pattern of dual tagged plasmids carrying APP-wt, D-CAA APP and APPΔ17 with ER, TGN, early endosomes and lysosomes in neuroblastoma cells. D-CAA APP CTFs exhibited aberrant colocalization with the endo-lysosomal compartments. This pattern was restored to APP wild type levels when APPΔ17 was transfected. Our study shows that removal of 49 amino acids from the APP protein does not affect intracellular localization of APP and reverses the abnormal cellular localization of Dutch APP.

MATERIAL AND METHODS

Antibodies and immunofluorescent stainings

For the colocalization analysis in iPSC-derived neuronal cells, neuronal precursor cells (NPCs) of one control and its isogenic D-CAA cell line (33), were first thawed and cultured in NPC medium (Stemcell Technologies), in a 6-well Matrigel (Corning) coated plate. NPC medium was refreshed every other day. When the cells reached confluency, 750.000 NPCs were plated in a 6-well PDL-laminin coated plate in StemDiff forebrain neuron differentiation medium (Stemcell technologies). The medium was refreshed daily for the next 7 days. Next, 250.000 cells were plated in PDL/laminin coated 12-well plates containing coverslips, in Brainphys neuronal medium (Stemcell technologies). At day 20 of neuronal differentiation, 30 µl of CellLight Reagents BacMam 2.0 (Life technologies) organelle markers; ER-RFP (C10591), Golgi-RFP (C10593) and early endosomes-RFP (C10587) were added in the culture medium and incubated O/N at 37°C and 5% CO_2. The next day cells were fixated with 4% PFA for 10 min at RT and washed three times with 1x PBS. The cells were subsequently used for immunofluorescent staining with antibodies against the N- and C- terminus of APP; to detect the N-terminus the APP monoclonal antibody 22C11 (# 14-9749-82, eBioscience,

Thermofisher scientific, RRID; AB_2572978, 1:500) and for the C-terminus the beta amyloid polyclonal antibody CT695 (#51-2700, Thermofisher scientific, RRID: AB_2533902, 1:250) were used. The immunofluorescent stainings were done in two different differentiation experiments. Images were acquired using the confocal SP8 microscope (Leica).

APP plasmid generation

Full length products were obtained by performing PCR using primers (Table 1) specific for the full length APP695 transcript. After extracting the PCR products of interest from the agarose gel, the fragments were purified and ligated into the pGEM-T Easy vector (Promega), using the 5'-A overhangs on the PCR products. Plasmids were subsequently digested with NotI and inserted into the PspOMI digested pAcGFP-C3 (Clontech, Mountain View, USA) vector. The moxGFP-APP695-ScarletI expression plasmids were obtained by insertion of the chemically synthesized (GenScript) APP exon1-moxGFP fragment into the AgeI/Acc65I digested pAcGFP1-APP695 constructs. This way AcGFP1 and the first exon of APP was removed and moxGFP was introduced in frame, immediately after the 17-amino acid signal peptide (SP) coding sequence of APP. Chemically synthesized (GenScript) fragments consisting of APP exon 15 to 17 (with the Dutch mutation or exon 16 missing) and the fusion tag mScarletI were subsequently introduced in frame downstream of the APP gene. This was then inserted into the moxGFP-APP695 plasmids with EcoRI restriction and ligation, where also the 3' end of the APP gene was replaced and the stop codon removed.

Transfection and immunofluorescent analysis

For the colocalization study in SHSY5Y cells, two transfection methods were used; lipofectamine 3000 and the adherent-cell electrode of the NEPA21 electroporation system. Human neuroblastoma SH-SY5Y cells were maintained in a 1:1 mixture of Minimum Essential Medium (MEM) (Gibco) and Ham's F-12 medium (Gibco) supplemented with 15% FBS, 1% Glutamax and 1% Penicillin/streptomycin. The SH-SY5Y cells were plated at 2.5 x 10^5 cells/well of a 12-well culture plate with coverslips and were differentiated with 10 μM retinoic acid (RA) five days prior to transfection. APP plasmids (2.5 ug concentration) were complexed with Lipofectamine 3000 in OptiMEM serum-free medium (Thermofisher) for 20 min and added drop-wise to the wells. OptiMEM medium was refreshed with serum-containing medium 4 hr after transfection.

Two experiments were performed with each transfection method. The two different transfection methods resulted in different efficiencies, with the NEPA21 electroporation being more efficient in plasmid transfection than lipofectamine 3000. However, the colocalization results were the same with both transfection methods, thus the single cell results from all four experiments were grouped for the analysis.

One day after transfection, SHSY5Y cells were fixated with 4% PFA, at RT for 10 min. Immunofluorescent staining was performed with cell organelle specific antibodies; ER was detected with the calreticulin antibody (Novus biologicals, # NBP1-47518, RRID: AB_10010469, 1:500), TGN was detected with the TGN46 monoclonal antibody 2F7.1 (Invitrogen, #MA3-063, RRID: AB_325484, 1:250), early endosomes were detected with the EEA1 antibody (BD biosciences, #610456, RRID:

AB_397829, 1:250) and lysosomes were detected with the CD107a (LAMP1) monoclonal antibody (eBioH4A3, #14-1079-80, Thermofisher scientific, RRID: AB_467426, 1:500). The cells were imaged with the confocal SP8 microscope (Leica).

Image analysis

Imaging of the iPSC-derived neuronal cells and SHSY5Y cells was performed on Leica SP8 confocal microscope. Confocal images were used as input for Cellprofiler to quantify the co-localization of each fragment with every organelle. For the colocalization analysis in iPSC-derived neuronal cells; for ER, a total of 35 images were analysed (20 control and 15 D-CAA), 17 images for Golgi (8 control and 9 D-CAA) and 20 images for early endosomes (7 control and 13 D-CAA). For the colocalization analysis in SHSY5Y; for ER, a total of 88 images were analyzed (21 APP-wt, 37 APP-D and 30 APPΔ17), 81 images for TGN (27 APP-wt, 29 APP-D and 25 APPΔ17), 65 images for endosomes (17 APP-wt, 28 APP-D and 20 APPΔ17) and 36 images for lysosomes (12 APP-wt, 12 APP-D and 12 APPΔ17). Due to size differences between the organelles, for every cell organelle a different pipeline was used. The typical diameter of ER foci was set between 6 and 30 pixel units, for Golgi between 2 and 30 pixel units and for endosomes and lysosomes between 2 and 25 pixel units. The typical diameter for NTFs and CTFs was set between 1 and 15 pixel units. The pipelines are available in the supplementary file.

RESULTS

APP N-terminal and C-terminal fragment distribution in organelles of iPSC neuronal cells

Control and D-CAA iPSC-derived neuronal cells were used for immunofluorescent co-localization analysis with antibodies against the N- and C-terminus of APP and organelle markers for ER, Golgi and early endosomes. There were no obvious differences regarding the number of neurons and astrocytes as well as in morphology between control and D-CAA iPSC-derived neuronal cultures. Twenty days after differentiation, we assessed the co-localization of the N- and C-terminal specific APP antibodies with the live cell organelle markers Cellight BacMam 2.0; ER-RFP, Golgi-RFP and early endosomes-RFP. The epitopes of the antibodies used to detect the APP-NTFs (22C11) and -CTFs (CT695) are presented in Figure 1A.

The staining pattern of the cell organelle markers was as reported previously (34-36), with the ER marker localizing in the cell soma around the nucleus, while Golgi and early endosomal markers were localized both in the cytoplasm and neuronal processes of control and D-CAA iPSC-derived neuronal cells (Figure 1B). The staining of ER, Golgi and endosomes in the cell soma colocalized mainly with APP-NTFs (Figure 1; C and D (ER), F and G (Golgi), I and J (endosomes), indicated by white dashed circles) in comparison with the endosome staining in the neuronal processes that mainly co-localized with both APP-NTFs and -CTFs (Figure 1; L, indicated by white dashed circles).

In control cells, the N- and C-terminal APP antibodies showed distinct staining patterns. Overall, APP-NTF and -CTF staining was found both in the cell soma and neuronal processes, however the APP-NTF showed a higher staining intensity in the cell soma while the APP CTF-specific antibody was more intense in the neuronal processes (Figure 1; E, G H and K, indicated by green and red

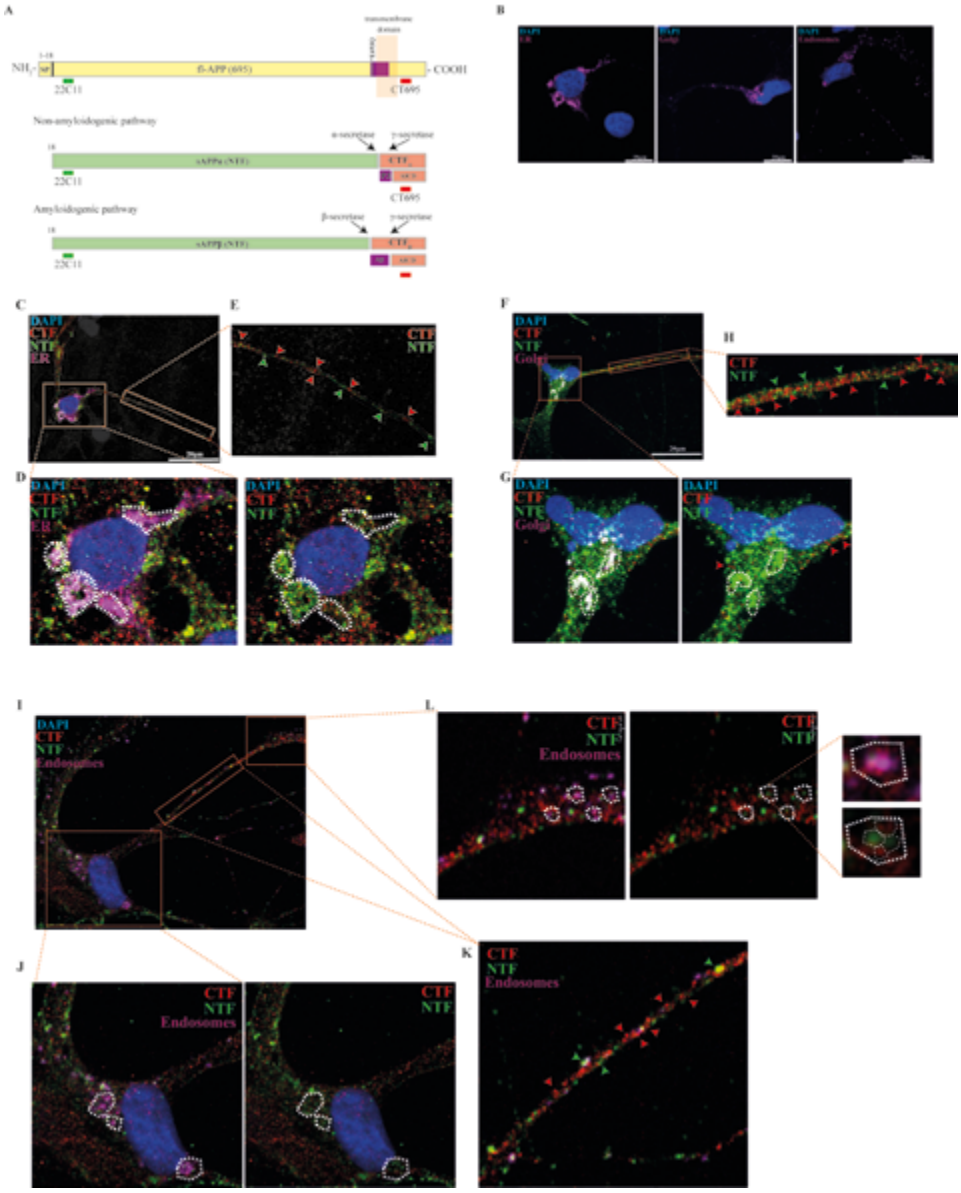

Figure 1. Endogenous APP cleavage fragment co-localization with cell organelles in control iPSC-derived neuronal cells. A. Schematic representation of full-length APP (695 aa) and the recognition sites of the N-terminus specific 22C11 APP antibody and the C-terminus specific CT695 APP antibody. The signal peptide (SP), Aβ domain (purple) and transmembrane domain are also depicted. Proteolytic cleavage fragments of APP via the non-amyloidogenic and amyloidogenic pathways are depicted with green (sAPPα, sAPPβ) or red color (CTFα, CTFβ and AICD), depending on the recognition site of the APP-specific antibody, B. Confocal images of control iPSC-derived neuronal cells immunofluorescently stained with live organelle markers against ER, Golgi and endosomes, C-L. Confocal images of control iPSC-derived neuronal cells immunofluorescently stained with APP NTF-specific antibody 22C11 (green), CTF-specific antibody CTF695 (red), DAPI (blue) and cell organelle markers (magenta).

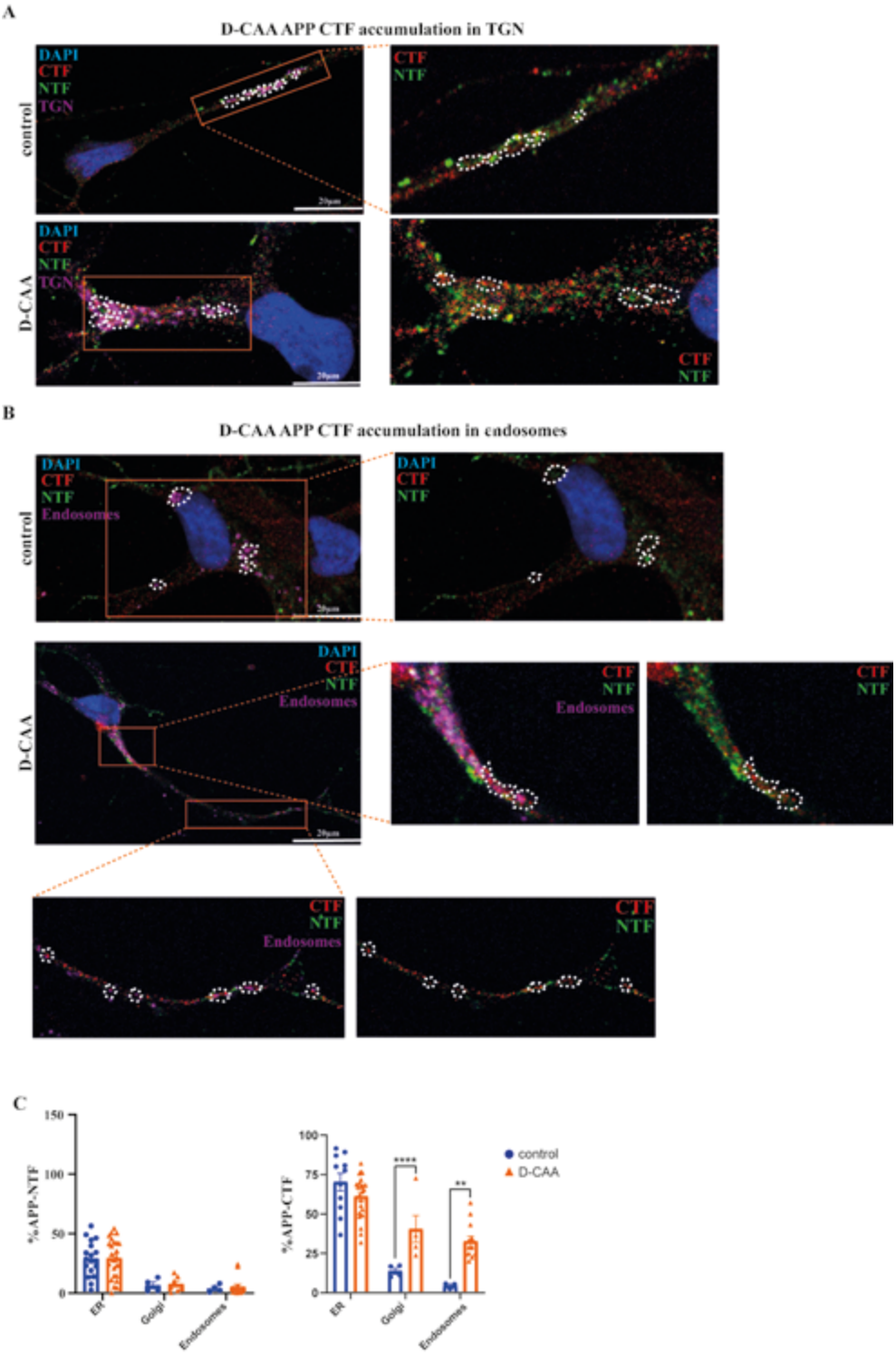
A
D-CAA APP CTF accumulation in TGN
control
D-CAA
DAPI
CTF
NTF
TGN
B
D-CAA APP CTF accumulation in endosomes
Endosomes
C
%APP-NTF
%APP-CTF
ER
Golgi
Endosomes
control
D-CAA
****
**

arrows). Moreover, in early endosomes we noticed a distinct staining pattern between NTFs and CTFs within an endosome. NTFs localized in the center of the endosome whereas CTFs where concentrated in the surface/rim of the early endosome (Figure 1; L).

Increased accumulation of the Dutch-type CTF in Golgi and early endosomal compartments of iPSC neuronal cells

The distribution of the APP-NTFs in ER, Golgi and endosomal compartments was similar in the control and D-CAA iPSC-derived neuronal cells. In the D-CAA cells, CTFs localized to the ER were similar to the control cells. However, the APP-CTFs were significantly more localized to the Golgi and endosomal compartments in D-CAA iPSC-derived neuronal cells compared to control cells (Figure 2; A and B indicated by white dashed circles). This shift in subcellular distribution of the D-CAA CTFs was confirmed after quantification. APP-NTF colocalization quantification revealed equal levels between control and D-CAA iPSC-derived neuronal cells in all organelles, whereas APP-CTF quantification exhibited a significantly increased colocalization in Golgi and endosomes of D-CAA iPSC-derived neuronal cells (Figure 2C). Both control and D-CAA CTFs showed similar localization levels within ER, suggesting that the synthesis of APP was similar in control and D-CAA cells.

The increased endogenous localization of the D-CAA CTFs within Golgi and endosomal compartments in iPSC-derived neuronal cells, led us to the hypothesis that altered cellular localization of the APP protein containing the Dutch mutation could be involved in disease pathology.

APP N-terminal and C-terminal fragment distribution in organelles of SHSY5Y cells

Next, we investigated if this change in cellular localization of D-CAA APP-CTFs could be confirmed with transient expression of dual-tagged APP constructs. In order to compare the cellular localization of wild-type and D-CAA APP, we generated expression constructs containing the APP-wt and the APP-D fused with a moxGFP tag at the N-terminus and an mScarletI tag in the C-terminus of APP (Figure 3A). The staining pattern of the ER-, TGN-, early endosome- and lysosome-specific antibodies were similar to that seen in the iPSC-derived neuronal cells. The ER-specific antibody (NBP1) showed cytoplasmic staining concentrated around the nucleus, the TGN-specific antibody (TGN38) displayed a staining pattern throughout the cell, although it showed smaller foci than the Golgi-RFP marker that was used in the iPSC-derived neuronal cells. The difference can be attributed to the fact that the Golgi-RFP is also a marker of the cis-Golgi membrane. The early

Figure 2. Accumulation of D-CAA APP-CTFs in TGN and endosomes A, B. Confocal images of control and D-CAA iPSC-derived neuronal cells immunofluorescently stained with APP NTF-specific antibody 22C11 (green), CTF-specific antibody CTF695 (red), DAPI (blue), Golgi-RFP (magenta) and/or endosomes-RFP (magenta), C. Quantification of APP-NTF and -CTF colocalization with ER, Golgi and endosomes in control (blue) and D-CAA (orange) iPSC-derived neuronal cells. Two independent neuronal differentiations were grouped in this graph. For the comparisons we used multiple t-tests with the post-hoc Holm-Sidak correction test.

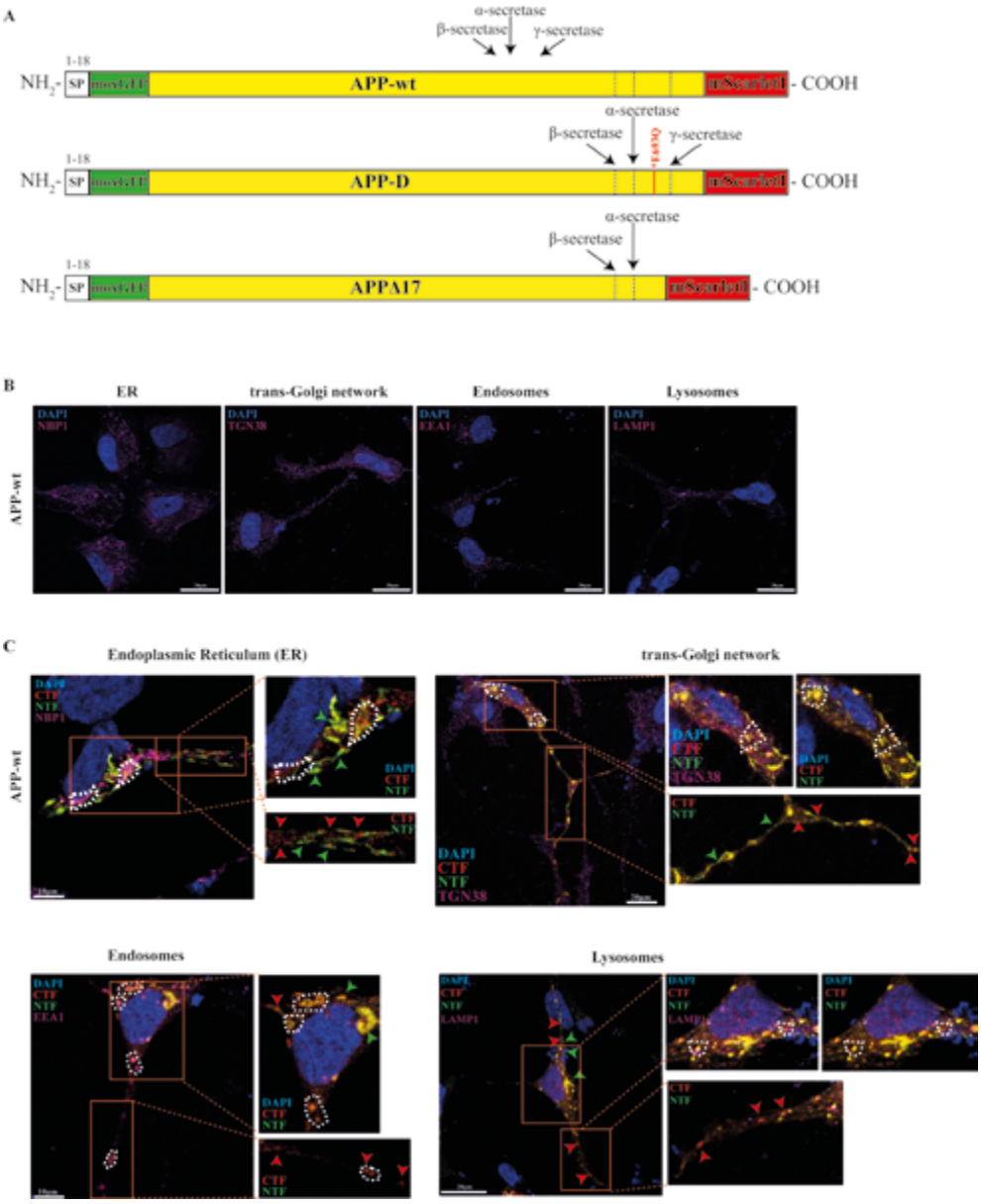

Figure 3. Subcellular localization of dual-tagged APP-wt plasmid. A. Schematic representation of the 3 dual-tagged plasmids carrying full-length APP (APP-wt), APP with the Dutch mutation E693Q (APP-D) and APPΔ17. The plasmids are tagged with moxGFP in the N-terminus, right after the SP sequence and with mScarletI in the C-terminus of APP. The α-, β- and γ-secretase cleavage sites are also depicted, B. Confocal images of immunofluorescently stained SHSY5Y cells with antibodies against NBP1 (ER), TGN38 (trans-Golgi) and EEA1 (early endosomes) and LAMP1 (lysosomes), C. Confocal images of APP-wt transfected SHSY5Y cells, immunofluorescently stained with antibodies against NBP1 (ER), TGN38 (trans-Golgi) and EEA1 (early endosomes) and LAMP1 (lysosomes), with APP-NTFs (green) and APP-CTFs (red).

endosome-specific antibody (EEA1) as well as the lysosome-specific antibody (LAMP1), showed a clear staining pattern throughout the cell and neuronal processes (Figure 3B).

In APP-wt transfected cells, APP-NTFs exhibited cytoplasmic localization mainly in the cell soma and less in the neuronal processes while APP-CTFs showed a localization pattern both at the cell soma and across the neuronal processes, in a similar fashion seen previously in the iPSC-derived neuronal cells (Figure 3C- indicated by green and red arrows). The APP-NTFs and -CTFs in the cell soma colocalized with ER, Golgi, early endosomes and lysosomes (Figure 3C- indicated by white dashed circles).

Increased accumulation of the Dutch-type CTF in Golgi and early endosomal compartments in SHSY5Y cells

Next, we studied the co-localization of APP-D NTFs and CTFs with the different organelle markers in transiently transfected SHSY5Y cells with dual tagged APP constructs. In SHSY5Y cells, APP-D CTFs showed an increased localization with endosomes and lysosomes compared to APP-wt CTFs (Figure 4 A and B – indicated by white dashed circles). There was also a difference in localization between APP-wt NTFs and APP-D NTFs in SHSY5Y cells, with APP-wt NTFs localizing around the nucleus and in the cytoplasm and APP-D NTFs appearing as larger foci in the cytoplasm and neuronal processes. This shift in subcellular distribution of the APP-D CTFs was confirmed after quantification of all confocal images, where we saw a significantly increased CTF accumulation in endosomes and lysosomes (Figure 4D). APP-D NTFs and CTFs showed similar colocalization in SHSY5Y cells and iPSC-derived neuronal cells for most organelles studied, except for Golgi where APP-D CTFs exhibited an increased tendency to colocalize with, however this was not significant.

The APP overexpression in SHSY5Y cells confirmed the endogenous localization in iPSC-derived neuronal cells, the significantly increased APP-D CTF localization in the endosomes and the increased localization of APP-D CTFs in the Golgi compartment that did not reach significance. Additionally a significantly increased colocalization of APP-D NTFs and CTFs with lysosomes was found.

APPΔ17 rescues the disrupted localization of the Dutch-type CTF

A previous study by our group showed the successful modification of APP pre-mRNA by removing exon 17 using an AON through splice modulation. This generates a new APP isoform, APPΔ17, that lacks the D-CAA mutation as well as part of the Aβ domain, reducing formation of the toxic Aβ peptide. Here, we hypothesized that APPΔ17 could reverse the increased localization of D-CAA APP-CTFs in different cell organelles. SHSY5Y cells were transfected with a dual-tagged plasmid carrying APPΔ17. We noticed a normalization of the significantly increased APP-D foci in endosomes and lysosomes, that looked similar to the APP-wt transfected cells (Figure 4C- indicated by dashed circles). Quantification of APPΔ17 CTFs showed a significant decrease in colocalization with Golgi, early endosomes and lysosomes when compared to APP-D CTFs and APP-wt CTFs (Figure 4D). Overall, these results indicate that the exon 17 targeting AON can successfully restore the phenotype seen in APP-D SHSY5Y cells.

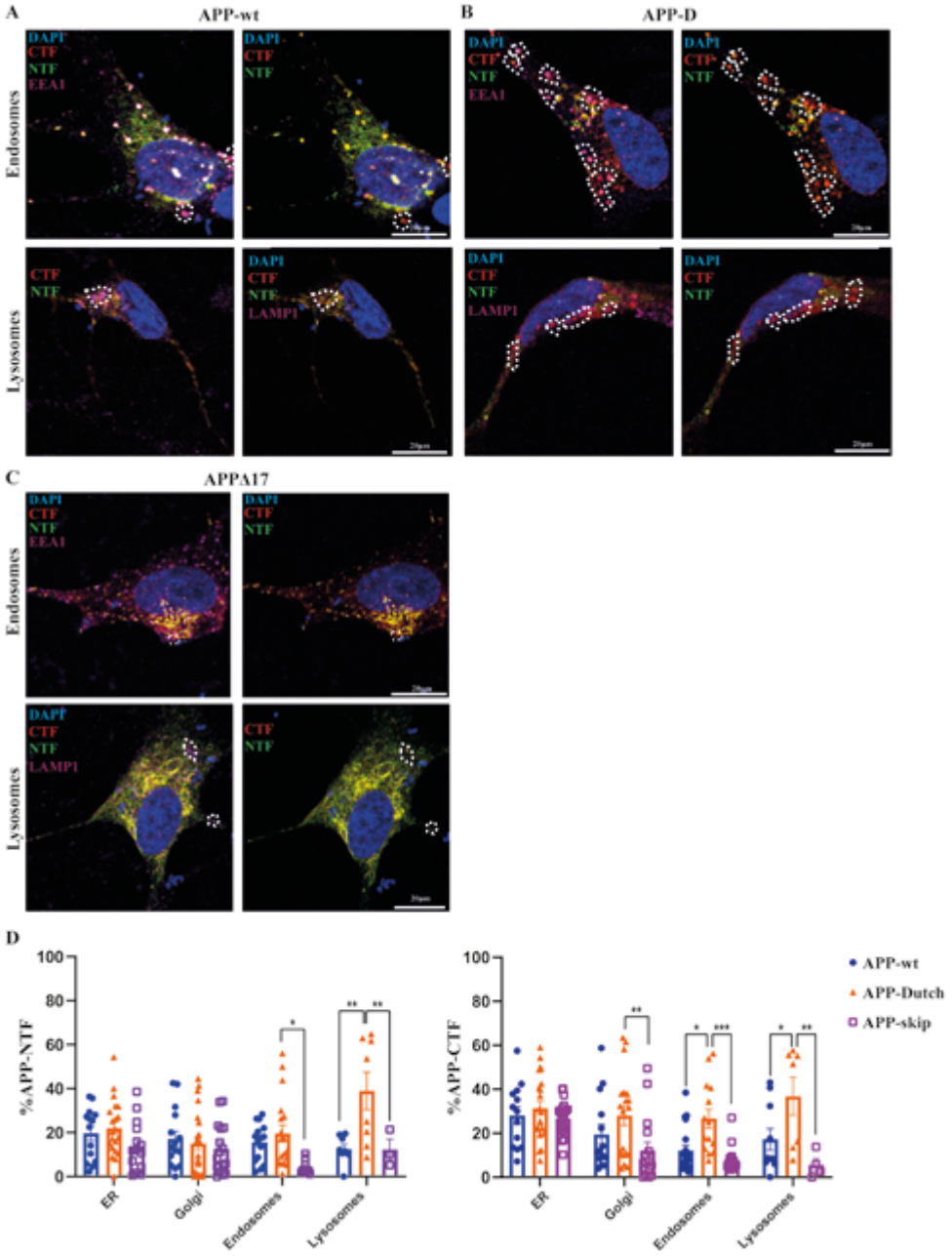

Figure 4. Accumulation of APP-D -CTFs in endosomes and lysosomes and phenotype restoration with APPΔ17, A-C. Confocal images of APP-wt, APP-D and APPΔ17 transfected SHSY5Y cells immunofluorescently stained with EEA1 (endosomes-magenta), LAMP1 (lysosomes-magenta) and DAPI (blue). E. Quantification of APP-NTF and –CTF colocalization with ER, Golgi, endosomes and lysosomes in APP-wt (blue), APP-D (orange) and APPΔ17 (magenta) transfected SHSY5Y cells. Four independent experiments (two transfections with lipofectamine and two NEPA21 electroporations) were grouped in each graph. For the comparisons we used multiple t-tests with the post-hoc Holm-Sidak correction test.

DISCUSSION

In the present study we looked into the subcellular localization of Dutch-type APP and compared it with the subcellular localization of wt-APP, both in an endogenous manner using patient-derived iPSC-derived neuronal cells, and using an overexpression system with APP plasmids in SHSY5Y cells. Dutch-type APP CTFs exhibited increased localization in Golgi and endolysosomal compartments. As our research interest extends to RNA-targeting therapeutics, we looked at the effect of the APPΔ17 isoform that is generated after AON treatment targeting exon 17 and leads to loss of the Dutch mutation and γ-secretase cleavage site. Indeed, APPΔ17 normalized the increased subcellular localization of Dutch-type APP.

Localization and trafficking of the APP protein is important for the generation of its proteolytic cleavage fragments that in turn are believed to modulate neuronal activity (37, 38). Many studies have shown that Aβ generation occurs in the endolysosomal pathway where γ-secretase physiologically resides, after APP is endocytosed from the plasma membrane (39-42). However, apart from APP endocytosis, the TGN network is also known to be a sorting station of APP to lysosomes, where Aβ will be finally produced (42-45). Neurons have been shown to be the major source of Aβ in the brain (46, 47), therefore the use of neuronal cell lines for the investigation of APP localization and trafficking is of great importance. In neurons, APP has been detected in most of the cell organelles. Previous immunolabeling studies have shown that when using N- and C-terminal specific APP antibodies it is possible to distinguish between APP-NTFs and -CTFs (48). When using simulated emission depletion (STED) microscopy in immunolabelled mouse hippocampal neurons it was shown that APP- NTFs and -CTFs are sorted in early endosomes. Our findings also indicated a clear separation between NTFs and CTFs in early endosomes, where NTFs localized in the center of the endosome and CTFs concentrated in the surface/rim of the endosome. However, we also found a separation between NTFs and CTFs in Golgi as well, meaning that both APP trafficking and sorting routes are present in iPSC-derived neuronal cells and SHSY5Y cells.

Increased D-CAA APP CTF localization to the Golgi and endolysosomal compartments suggests that the Dutch mutation affects proper APP processing and trafficking. The Dutch mutation is located in the juxtamembrane region of the APP protein, upstream of the APP transmembrane domain and is part of the cholesterol binding domain (CBD) motif in APP (29). Furthermore, it has been shown that only mutations within the CBD domain (G700A and I703A) affected the surface distribution of APP leading to the conclusion that APP's affinity to bind cholesterol could directly affect APP internalization or prevent externalization (49). Since CAA has been also associated with impaired lipid metabolism (50, 51), future studies on APP trafficking and processing should include the role of lipoproteins.

In this study we looked at localization of both the endogenous APP and D-CAA APP, in iPSC-derived neuronal cells and overexpressed APP in the SHSY5Y cell line, and showed similar results with the two different cell models. Based on our results it is evident that in both the endocytic and secretory APP sorting pathways D-CAA APP is aberrantly localized. Although in general, neither β- nor γ-secretase are active in early secretory compartments like the ER and Golgi (19), there are data showing that the amyloidogenic pathway can also occur in these compartments (52-54).

The increased localization of D-CAA APP CTFs in both Golgi and early endosomes, suggests that the Dutch mutation could favor proteolytic amyloidogenic cleavage in these organelles, as they have been shown before to bidirectionally communicate with transport vesicles during APP processing (55). Another interesting finding of our study was the significantly increased localization of both D-CAA NTFs and CTFs within lysosomes. This could be attributed either to aberrant recycling of APP and APP cleavage products or a rapid transport of APP-CTFs from Golgi to lysosomes where they are further cleaved by γ-secretase (21). Cleavage of APP in the lysosomes has been shown previously in the study of Lorenzen et al. where they suggested a novel pathway in which APP is transported rapidly from the cell surface to lysosomes bypassing endosomes for proteolytic cleavage (56). An increased accumulation of APP CTFs in endosomes and lysosomes has been shown before in cell and mouse models of AD (57-59), further supporting our hypothesis for APP processing impairment upstream of the Aβ deposition. To more thoroughly investigate the trafficking and localization of the different APP cleavage fragments, future studies will include high-resolution live-cell microscopy.

Our combined results suggest that the D-APP affects both the secretory and endocytic pathways. During the first, APP can be aberrantly processed in Golgi, generating a large amount of APP-CTFs that are then transported for further processing to endosomes and/or lysosomes, while in the latter plasma membrane APP can rapidly traffic to lysosomes, where it is further processed (Figure 5).

Recently, our group showed that an AON targeting exon 17, generated a new APP isoform (APPΔ17) that lacks the Aβ domain leading to lower secreted Aβ40 and Aβ42 (32). In the current study we show not only that APPΔ17 and APP-wt have a similar distribution in the ER, Golgi, endosomal and lysosomal compartments but that APPΔ17 also reverses the increased APP-D CTF accumulation in endosomes and the increased NTF and CTF accumulation in lysosomes. Exon 17 encodes for part of the APP juxtamembrane and transmembrane domains, therefore the APPΔ17 isoform will lack parts of these domains. Part of the CBD will also be absent in the APPΔ17 isoform meaning the proteolytic cleavage could be affected. We hypothesize that due to loss of these domains APPΔ17 is most likely is not membrane-bound but soluble, and therefore cannot accumulate in the cell. Further functional studies need to be done to determine the properties of this isoform and its cleavage fragments.

CONCLUSION

In this study we showed that APP carrying the Dutch mutation (APP-D) shows different subcellular localization than APP-wt, suggesting that there is an impairment of APP processing and/or APP trafficking in D-CAA. We also showed the feasibility of removal of exon 17 from the APP pre-mRNA as a therapeutic approach for D-CAA. Apart from preventing formation of the toxic amyloid beta fragments we here show that this approach also normalizes the impaired localization phenotype of APP-D. To investigate the trafficking of APP-D, as well as to look into the exact trafficking of the APPΔ17 isoform, further studies with high-resolution live cell confocal microscopy will provide more information.

CONFLICT OF INTEREST

The authors declare no conflict of interest

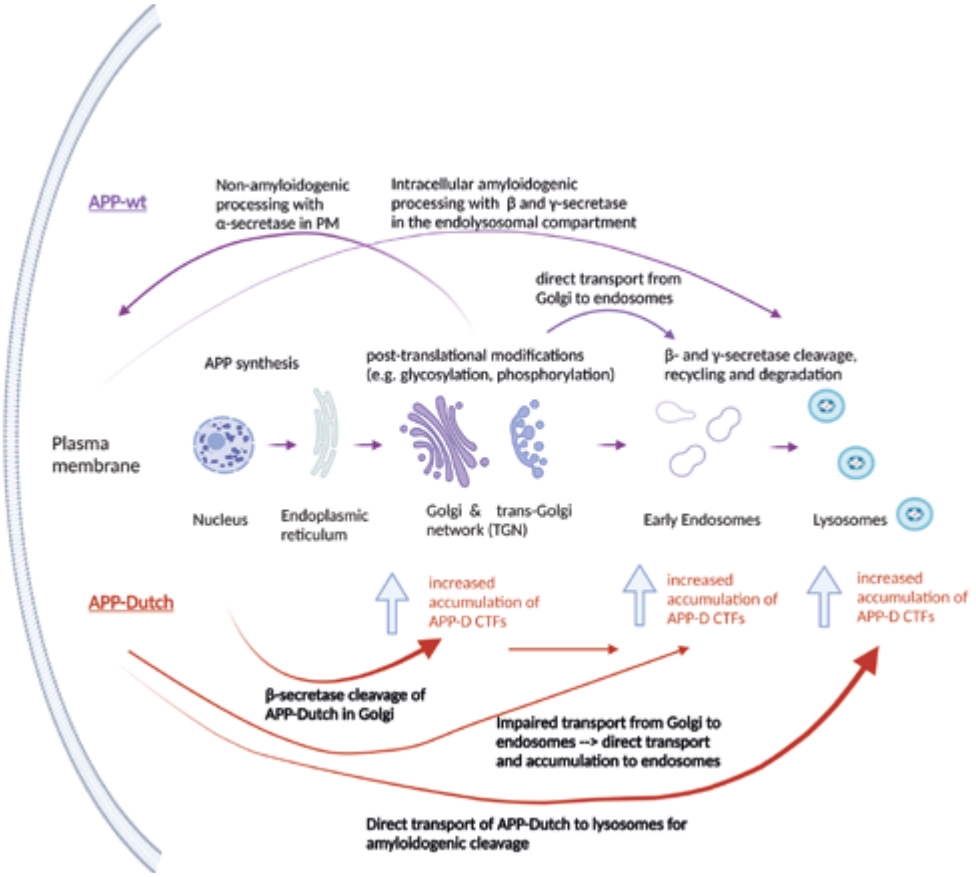

Figure 5. Proposed trafficking pathway of APP-wt and APP-Dutch isoforms. After APP-wt synthesis in the nucleus, APP translocates to the ER and enters the Golgi where it is post-translationally modified. From Golgi it can be recycled back to the plasma membrane where it will be cleaved by α-secretase in the non-amyloidogenic pathway or it can be directly transported to the endolysosomal system where it will be cleaved by β- and γ- secretases. When APP-D is transported to Golgi, there is an increased accumulation of CTFs meaning that β-secretase cleavage of APP happens in the Golgi compartments. After that, CTFs are transported to the endolysosomal system for γ-secretase cleavage and degradation. Another hypothesis is that APP-D could be also directly transported from the plasma membrane to the endolysosomal system for amyloidogenic cleavage.

AUTHOR CONTRIBUTIONS

ED performed the experiments, did the analysis and wrote the manuscript.

BP assisted with the experimental design and performed the experiments.

LvdG assisted with the analysis.

WvRM conceptualized the study and reviewed the manuscript.

FUNDING

This study was funded by Amylon Therapeutics B.V.

ACKNOWLEDGMENTS

SUPPLEMENTARY MATERIAL

Supplementary Material should be uploaded separately on submission, if there are Supplementary Figures, please include the caption in the same file as the figure. Supplementary Material templates can be found in the Frontiers Word Templates file.

Please see the Supplementary Material section of the Author guidelines for details on the different file types accepted.

REFERENCES

1. Bornebroek M, Haan J, Maat-Schieman ML, Van Duinen SG, Roos RA. Hereditary cerebral hemorrhage with amyloidosis-Dutch type (HCHWA-D): I--A review of clinical, radiologic and genetic aspects. Brain Pathol. 1996;6(2):111-4.
2. Bornebroek M, Haan J, Van Duinen SG, Maat-Schieman ML, Van Buchem MA, Bakker E, et al. Dutch hereditary cerebral amyloid angiopathy: structural lesions and apolipoprotein E genotype. Ann Neurol. 1997;41(5):695-8.
3. Levy E, Carman MD, Fernandez-Madrid IJ, Power MD, Lieberburg I, van Duinen SG, et al. Mutation of the Alzheimer's disease amyloid gene in hereditary cerebral hemorrhage, Dutch type. Science. 1990;248(4959):1124-6.
4. Kamp JA, Moursel LG, Haan J, Terwindt GM, Lesnik Oberstein SAMJ, van Duinen SG, et al. Amyloid β in hereditary cerebral hemorrhage with amyloidosis-Dutch type. Reviews in the Neurosciences. 2014;25(5).
5. Zheng H, Koo EH. Biology and pathophysiology of the amyloid precursor protein. Molecular Neurodegeneration. 2011;6(1):27.
6. Dawkins E, Small DH. Insights into the physiological function of the β-amyloid precursor protein: beyond Alzheimer's disease. Journal of Neurochemistry. 2014;129(5):756-69.
7. Habib A, Sawmiller D, Tan J. Restoring Soluble Amyloid Precursor Protein α Functions as a Potential Treatment for Alzheimer's Disease. J Neurosci Res. 2017;95(4):973-91.
8. Mockett BG, Richter M, Abraham WC, Müller UC. Therapeutic Potential of Secreted Amyloid Precursor Protein APPsα. Frontiers in Molecular Neuroscience. 2017;10(30).
9. Gakhar-Koppole N, Hundeshagen P, Mandl C, Weyer SW, Allinquant B, Müller U, et al. Activity requires soluble amyloid precursor protein α to promote neurite outgrowth in neural stem cell-derived neurons via activation of the MAPK pathway. European Journal of Neuroscience. 2008;28(5):871-82.
10. Taylor CJ, Ireland DR, Ballagh I, Bourne K, Marechal NM, Turner PR, et al. Endogenous secreted amyloid precursor protein-alpha regulates hippocampal NMDA receptor function, long-term potentiation and spatial memory. Neurobiol Dis. 2008;31(2):250-60.
11. Zhang H, Ma Q, Zhang YW, Xu H. Proteolytic processing of Alzheimer's beta-amyloid precursor protein. J Neurochem. 2012;120 Suppl 1:9-21.
12. Nikolaev A, McLaughlin T, O'Leary DD, Tessier-Lavigne M. APP binds DR6 to trigger axon pruning and neuron death via distinct caspases. Nature. 2009;457(7232):981-9.
13. Charidimou A, Friedrich JO, Greenberg SM, Viswanathan A. Core cerebrospinal fluid biomarker profile in cerebral amyloid angiopathy: A meta-analysis. Neurology. 2018;90(9):e754-e62.
14. Słomnicki LP, Leśniak W. A putative role of the Amyloid Precursor Protein Intracellular Domain (AICD) in transcription. Acta Neurobiol Exp (Wars). 2008;68(2):219-28.
15. Shu R, Wong W, Ma QH, Yang ZZ, Zhu H, Liu FJ, et al. APP intracellular domain acts as a transcriptional regulator of miR-663 suppressing neuronal differentiation. Cell Death & Disease. 2015;6(2):e1651-e.
16. Chow VW, Mattson MP, Wong PC, Gleichmann M. An overview of APP processing enzymes and products. Neuromolecular medicine. 2010;12(1):1-12.
17. Zhang X, Song W. The role of APP and BACE1 trafficking in APP processing and amyloid-β generation. Alzheimer's Research & Therapy. 2013;5(5):46.
18. SELKOE DJ, YAMAZAKI T, CITRON M, PODLISNY MB, KOO EH, TEPLOW DB, et al. The Role of APP Processing and Trafficking Pathways in the Formation of Amyloid β-Proteina. Annals of the New York Academy of Sciences. 1996;777(1):57-64.
19. Haass C, Kaether C, Thinakaran G, Sisodia S. Trafficking and proteolytic processing of APP. Cold Spring Harb Perspect Med. 2012;2(5):a006270.
20. Muresan V, Ladescu Muresan Z. Amyloid-β precursor protein: Multiple fragments, numerous transport routes and mechanisms. Exp Cell Res. 2015;334(1):45-53.
21. Tam JHK, Seah C, Pasternak SH. The Amyloid Precursor Protein is rapidly transported from the Golgi apparatus to the lysosome and where it is processed into beta-amyloid. Molecular Brain. 2014;7(1):54.
22. Haass C, Schlossmacher MG, Hung AY, Vigo-Pelfrey C, Mellon A, Ostaszewski BL, et al. Amyloid β-peptide is produced by

cultured cells during normal metabolism. Nature. 1992;359(6393):322-5.
23. Kins S, Lauther N, Szodorai A, Beyreuther K. Subcellular trafficking of the amyloid precursor protein gene family and its pathogenic role in Alzheimer's disease. Neurodegener Dis. 2006;3(4-5):218-26.
24. Shao W, Peng D, Wang X. Genetics of Alzheimer's disease: From pathogenesis to clinical usage. J Clin Neurosci. 2017;45:1-8.
25. Ren Z, Schenk D, Basi GS, Shapiro IP. Amyloid β-Protein Precursor Juxtamembrane Domain Regulates Specificity of γ-Secretase-dependent Cleavages. Journal of Biological Chemistry. 2007;282(48):35350-60.
26. Sato M, Sato K, Nakano A. Endoplasmic reticulum localization of Sec12p is achieved by two mechanisms: Rer1p-dependent retrieval that requires the transmembrane domain and Rer1p-independent retention that involves the cytoplasmic domain. Journal of Cell Biology. 1996;134(2):279-93.
27. Munro S. A comparison of the transmembrane domains of Golgi and plasma membrane proteins. Biochemical Society Transactions. 1995;23(3):527-30.
28. Opat AS, van Vliet C, Gleeson PA. Trafficking and localisation of resident Golgi glycosylation enzymes. Biochimie. 2001;83(8):763-73.
29. Barrett PJ, Song Y, Van Horn WD, Hustedt EJ, Schafer JM, Hadziselimovic A, et al. The Amyloid Precursor Protein Has a Flexible Transmembrane Domain and Binds Cholesterol. Science. 2012;336(6085):1168-71.
30. Hanbouch L, Schaack B, Kasri A, Fontaine G, Gkanatsiou E, Brinkmalm G, et al. Specific Mutations in the Cholesterol-Binding Site of APP Alter Its Processing and Favor the Production of Shorter, Less Toxic Aβ Peptides. Molecular Neurobiology. 2022;59(11):7056-73.
31. Zhang J, Ye W, Wang R, Wolfe MS, Greenberg BD, Selkoe DJ. Proteolysis of chimeric beta-amyloid precursor proteins containing the Notch transmembrane domain yields amyloid beta-like peptides. J Biol Chem. 2002;277(17):15069-75.
32. Daoutsali E, Hailu TT, Buijsen RAM, Pepers BA, van der Graaf LM, Verbeek MM, et al. Antisense Oligonucleotide-Induced Amyloid Precursor Protein Splicing Modulation as a Therapeutic Approach for Dutch-Type Cerebral Amyloid Angiopathy. Nucleic Acid Therapeutics. 2021.
33. Daoutsali E, Pepers BA, Stamatakis S, van der Graaf LM, Terwindt GM, Parfitt DA, et al. Amyloid beta accumulations and enhanced neuronal differentiation in cerebral organoids of Dutch-type cerebral amyloid angiopathy patients. Frontiers in Aging Neuroscience. 2023;14.
34. Roderick HL, Campbell AK, Llewellyn DH. Nuclear localisation of calreticulin in vivo is enhanced by its interaction with glucocorticoid receptors. FEBS Letters. 1997;405(2):181-5.
35. Mairhofer M, Steiner M, Salzer U, Prohaska R. Stomatin-like Protein-1 Interacts with Stomatin and Is Targeted to Late Endosomes*. Journal of Biological Chemistry. 2009;284(42):29218-29.
36. Storrie B, White J, Röttger S, Stelzer EHK, Suganuma T, Nilsson T. Recycling of Golgi-resident Glycosyltransferases through the ER Reveals a Novel Pathway and Provides an Explanation for Nocodazole-induced Golgi Scattering. Journal of Cell Biology. 1998;143(6):1505-21.
37. Cirrito JR, Kang J-E, Lee J, Stewart FR, Verges DK, Silverio LM, et al. Endocytosis Is Required for Synaptic Activity-Dependent Release of Amyloid-β In Vivo. Neuron. 2008;58(1):42-51.
38. Wang H, Megill A, He K, Kirkwood A, Lee H-K. Consequences of Inhibiting Amyloid Precursor Protein Processing Enzymes on Synaptic Function and Plasticity. Neural Plasticity. 2012;2012:272374.
39. Schrader-Fischer G, Paganetti PA. Effect of alkalizing agents on the processing of the β-amyloid precursor protein. Brain Research. 1996;716(1):91-100.
40. Bagshaw RD, Pasternak SH, Mahuran DJ, Callahan JW. Nicastrin is a resident lysosomal membrane protein. Biochemical and Biophysical Research Communications. 2003;300(3):615-8.
41. Pasternak SH, Bagshaw RD, Guiral M, Zhang S, Ackerley CA, Pak BJ, et al. Presenilin-1, Nicastrin, Amyloid Precursor Protein, and γ-Secretase Activity Are Co-localized in the Lysosomal Membrane*. Journal of Biological Chemistry. 2003;278(29):26687-94.
42. Toh Wei H, Gleeson Paul A. Dysregulation of intracellular trafficking and endosomal sorting in Alzheimer's disease: controversies

and unanswered questions. Biochemical Journal. 2016;473(14):1977-93.
43. Capell A, Meyn L, Fluhrer R, Teplow DB, Walter J, Haass C. Apical Sorting of β-Secretase Limits Amyloid β-Peptide Production*. Journal of Biological Chemistry. 2002;277(7):5637-43.
44. Andersen OM, Reiche J, Schmidt V, Gotthardt M, Spoelgen R, Behlke J, et al. Neuronal sorting protein-related receptor sorLA/LR11 regulates processing of the amyloid precursor protein. Proceedings of the National Academy of Sciences. 2005;102(38):13461-6.
45. Tan JZA, Gleeson PA. The role of membrane trafficking in the processing of amyloid precursor protein and production of amyloid peptides in Alzheimer's disease. Biochimica et Biophysica Acta (BBA) - Biomembranes. 2019;1861(4):697-712.
46. Zhao J, Paganini L, Mucke L, Gordon M, Refolo L, Carman M, et al. β-Secretase Processing of the β-Amyloid Precursor Protein in Transgenic Mice Is Efficient in Neurons but Inefficient in Astrocytes *. Journal of Biological Chemistry. 1996;271(49):31407-11.
47. Calhoun ME, Burgermeister P, Phinney AL, Stalder M, Tolnay M, Wiederhold K-H, et al. Neuronal overexpression of mutant amyloid precursor protein results in prominent deposition of cerebrovascular amyloid. Proceedings of the National Academy of Sciences. 1999;96(24):14088-93.
48. Muresan V, Varvel NH, Lamb BT, Muresan Z. The cleavage products of amyloid-beta precursor protein are sorted to distinct carrier vesicles that are independently transported within neurites. J Neurosci. 2009;29(11):3565-78.
49. DelBove CE, Strothman CE, Lazarenko RM, Huang H, Sanders CR, Zhang Q. Reciprocal modulation between amyloid precursor protein and synaptic membrane cholesterol revealed by live cell imaging. Neurobiology of Disease. 2019;127:449-61.
50. Bonaterra-Pastra A, Fernández-de-Retana S, Rivas-Urbina A, Puig N, Benítez S, Pancorbo O, et al. Comparison of Plasma Lipoprotein Composition and Function in Cerebral Amyloid Angiopathy and Alzheimer's Disease. Biomedicines. 2021;9(1):72.
51. Reed B, Villeneuve S, Mack W, DeCarli C, Chui HC, Jagust W. Associations between serum cholesterol levels and cerebral amyloidosis. JAMA Neurol. 2014;71(2):195-200.
52. Muresan V, Muresan Z. A persistent stress response to impeded axonal transport leads to accumulation of amyloid-β in the endoplasmic reticulum, and is a probable cause of sporadic Alzheimer's disease. Neurodegener Dis. 2012;10(1-4):60-3.
53. Skovronsky DM, Doms RW, Lee VM. Detection of a novel intraneuronal pool of insoluble amyloid beta protein that accumulates with time in culture. J Cell Biol. 1998;141(4):1031-9.
54. Cook DG, Forman MS, Sung JC, Leight S, Kolson DL, Iwatsubo T, et al. Alzheimer's A beta(1-42) is generated in the endoplasmic reticulum/ intermediate compartment of NT2N cells. Nat Med. 1997;3(9):1021-3.
55. Choy RW-Y, Cheng Z, Schekman R. Amyloid precursor protein (APP) traffics from the cell surface via endosomes for amyloid β (Aβ) production in the trans-Golgi network. Proceedings of the National Academy of Sciences of the United States of America. 2012;109(30):E2077-E82.
56. Lorenzen A, Samosh J, Vandewark K, Anborgh PH, Seah C, Magalhaes AC, et al. Rapid and direct transport of cell surface APP to the lysosome defines a novel selective pathway. Mol Brain. 2010;3:11.
57. Lauritzen I, Pardossi-Piquard R, Bauer C, Brigham E, Abraham J-D, Ranaldi S, et al. The β-Secretase-Derived C-Terminal Fragment of βAPP, C99, But Not Aβ, Is a Key Contributor to Early Intraneuronal Lesions in Triple-Transgenic Mouse Hippocampus. The Journal of Neuroscience. 2012;32(46):16243-55.
58. Lauritzen I, Pardossi-Piquard R, Bourgeois A, Pagnotta S, Biferi M-G, Barkats M, et al. Intraneuronal aggregation of the β-CTF fragment of APP (C99) induces Aβ-independent lysosomal-autophagic pathology. Acta Neuropathologica. 2016;132(2):257-76.
59. Jiang Y, Sato Y, Im E, Berg M, Bordi M, Darji S, et al. Lysosomal Dysfunction in Down Syndrome Is APP-Dependent and Mediated by APP-βCTF (C99). The Journal of Neuroscience. 2019;39(27):5255-68.